DRFC/CAD

EUR-CEA-FC-1705

On the Role of Ion Heating in ICRF-heated Discharges in Tore Supra

L G Eriksson, G. Hoang, V Bergeaud

September 2000

On the Role of Ion Heating in ICRF-heated Discharges in Tore Supra

L.-G. ERIKSSON, G. T. HOANG, V. BERGEAUD

Association EURATOM-CEA sur la Fusion Contrôlée, CEA Cadarache,

F-13108 St. Paul lez Durance, France

Abstract. The effect of bulk ion heating in Tore Supra has been investigated by studying discharges with varying concentrations of minority ions during ICRF hydrogen minority heating in Deuterium/^{4}He plasmas. As expected, the level of bulk ion heating is found to increase with the minority concentration. Higher levels of ion heating are shown to be accompanied by two significant effects: an improved energy confinement and a strong influence on the plasma rotation.

1. INTRODUCTION

It is desirable to have a significant fraction of ion heating during auxiliary heating of fusion plasmas. An important reason for this is of course that the fusion reactivity of the reacting ion species depends strongly on the ion temperature. Thus, in choosing an auxiliary heating scenario for a reactor it is important to consider its potential for providing ion heating. The use of intense waves in the Ion Cyclotron Range of Frequencies (ICRF) is one of the main methods considered for heating of fusion reactors. The utility of this heating method has been demonstrated in many tokamak experiments around the world [1, 2, 3]. However, very often the resonating (i.e. absorbing) ions become very energetic and transfer most of the absorbed ICRF power to bulk electrons ions via collisions. Consequently, special care has to be taken in designing ICRF heating scenarios for a reactor [4]. In recent Tore experiments, regimes with various levels of bulk ion heating during application of ICRF waves have been explored (see Ref. [5] for machine details). We report on these experiments and the observed influence of ion heating on the plasma performance. In particular, the energy confinement is found to

improve at higher levels of ion heating. In addition, the level of ion heating appears to have a strong influence on the plasma rotation.

Let us first review some basic features of ICRF heating. Most of these are well known in the ICRF community and were described in Stix's seminal 1975 paper [6], here we discus them for completeness. There are two main scenarios for ICRF heating: heating of a minority species at its fundamental ion cyclotron frequency and heating at the second harmonic (or higher harmonic) of the ion cyclotron frequency of a majority species. In the case of fundamental minority heating, the ICRF power per resonating particle is often high. As a consequence, the absorbing ions are frequently accelerated to high velocities, and ions in the MeV range are routinely produced in present day experiments [7, 8]. These energetic ions collide mainly with electrons and the ICRF power is therefore to a large extent transferred to the bulk plasma electrons rather than the bulk ions. On the other hand, in the case of second harmonic heating of a majority species, the ICRF power per resonating ions is more moderate. However, the absorption mechanism during second harmonic heating is a Finite Larmor Radius (FLR) effect. The efficiency of the wave particle interaction is therefore better at high perpendicular velocities. As a consequence, high power second harmonic ICRF heating tends to create a high energy tail on the distribution function of the resonating ions consisting of relatively few very energetic ions. Predominant bulk electron heating will in this case also prevail.

In order to improve the bulk ion heating it is necessary to limit the high energy tail on the resonating ion distribution created by the ICRF heating. In fact the averaged energy of the resonating ions should be kept below or around the critical velocity, v_c, to achieve good ion heating. The critical velocity is the velocity at which the collisional power transfers to the ions and electrons are equally strong, and it is given by [6],

$$\frac{1}{2}\mathrm{m}v_c^2 = 14.8kT_e \left(\frac{A^{3/2}}{n_e}\right)_j \left(\frac{n_j Z_j^2}{A_j}\right)^{2/3},$$

where A is the atomic mass of the resonating species, A_j is the atomic masses of the ion species in the plasma, n_j their densities. For hydrogen minority heating in a typical Tore Supra discharge ($T_e = 4keV$) this gives an energy of the order of 50 - 100 keV. There are several ways to limit the energy of the resonating ions, for example: increasing the density of the resonating ions, see e.g. [1] for experimental verification; increasing the plasma density; moving the cyclotron resonance layer off axis. In the case of fundamental minority heating, increasing the concentration of the minority ions will come at the cost of a reduced absorption efficiency of the ICRF waves and an increased fraction of power being mode converted into ion Bernstein waves, which are thought to damp mainly on bulk electrons. Experiments with high concentration minority heating at JET [9] have, however, shown that one can use quite high concentrations of minority ions and still achieve reasonably effective damping on them. This is particularly true of the scenario with hydrogen minority heating in deuterium and/or He^4. This is also the scenario we have used in Tore Supra. By moving the resonance of axis the ICRF power can be absorbed in a greater volume, thus decreasing the power per absorbing ion. The drawback of this method is of course that the power is not absorbed in the centre of the plasma, which is normally preferable. In the Tore Supra experiments, we have used a combination of these methods to study the effect of improved ion heating on the performance.

2. EXPERIMENTAL RESULTS

The basic scenario used in the Tore Supra experiments reported here was hydrogen minority heating in a mixture of deuterium and ^{4}He. As we have remarked in the introduction, the minority concentration plays a crucial role for the ion heating fraction and it is necessary to determine it with reasonable accuracy to interpret the experimental results properly. In the next sub section we briefly describe the method we have used to determine the concentration and then proceed to review the experimental results obtained for various concentrations.

2.1 Determination of the hydrogen concentration

In order to determine the hydrogen concentration we use the passive charge exchange measurements [10], which measure both the hydrogen flux and the deuterium flux. The hydrogen flux, Φ_H, can be written as,

$$\Phi_H(E) = \int n_H n_0 f(E) G(E) dl \ ,$$

where n_H is the hydrogen density, n_0, is the density of neutrals, E is the energy of the escaping hydrogen atoms, $f(E)$, is the energy distribution of hydrogen ions, $G(E)$ is a function which accounts for neutralisation cross section, the aperture of the instrument etc., and the integral is carried out along a line of sight through the plasma. Owing to the rapid decrease of the neutral density away from the plasma boundary towards the centre of the plasma, the hydrogen flux, especially at low energies, is strongly weighted towards the plasma boundary. Assuming a Maxwellian distribution of hydrogen ions, which is appropriate towards the plasma periphery, we can write

$$\ln \Phi(E) = \ln(n_H n_0) - \frac{E}{T} + \ln G(E)$$

By using this expression and determining the slope of the experimentally measured flux in the low energy region we could in principle calculate the hydrogen concentration. However, the neutral density is not known. In order to overcome this problem we repeat the same procedure for the deuterium flux, and can normalise out the neutral density by taking the ratio n_H / n_D .

In a plasma with deuterium as the single majority species we can now calculate the densities for the relevant ion species from the measurements of Z_{eff} and the ratio of n_H / n_D (assuming we have a rough idea of the dominating impurities in the plasma). However, in a plasma with a mixture of deuterium and ^{4}He it is also necessary to estimate the deuterium density. This can be done by using the measurements of the DD neutron rate and the central ion temperature. By assuming the deuterium density to have the same profile shape as the electron density we

can, together with modelling of the shape of the ion temperature profile, determine the deuterium density so that the measured neutron rate is reproduced.

The procedure described above gives us a reasonable estimate of the magnitude of the hydrogen concentration in Tore Supra discharges. However, it should be remarked that the error bars are quite large. Especially since the method described above gives an estimate for the hydrogen concentration in the outer part of the plasma, while the absorption of the ICRF waves takes place more centrally. This should be kept in mind when analysing the experimental data.

2.2 Comparison between to discharges with high and low hydrogen concentrations

In order to illustrate the effect of increased hydrogen concentration, and thereby improved ion heating, we compare two Tore Supra discharges with different hydrogen concentration, #TS21044 and #TS23967 which are well matched in terms of heating power. The plasma current and the central magnetic field was 1.3MA and 3.6T respectively in both discharges. Furthermore, the frequency was 57 MHz and dipole phasing of the ICRF antennas was used, peaking the toroidal mode number spectrum around N≈35 (for a description of the ICRF system see Ref. [11]). In #TS21044 the hydrogen concentration was around $n_H / n_e \cup 6\%$ during the ICRF heating phase, whereas it was about 2.5% for #TS23967. Equilibrium reconstruction shows that the cyclotron resonance was about 10cm on the high field side of the magnetic axis, with #TS21044 being a few cm centimetres more off axis than #TS23967. An overview of the two discharges is shown in Fig. 1. As can be seen, the ion and electron temperatures (measured by an x-ray crystal and ECE) are almost equal for the high concentration discharge whereas the ion temperature increase is very modest for the low the concentration discharge. Thus, there are clear signs of improved ion heating in the high concentration discharge. In fact the overall confinement of the plasma is also improved, Fig. 1, the trace of the diamagnetic stored energy is well above the ITER-L97 L-mode scaling law [12] for the high concentration discharge (note that the no corrections for ripple losses have been made in the evaluation of the scaling law, see section 3 below). On the other hand, the low

concentration discharge remains in L-mode. In addition, despite of the fact that the total electron heating should have been lower in the high concentration discharge, the stored electron energy is higher for this discharge than in the low concentration one. This can also be clearly seen in the electron pressure profiles, Fig. 2. Despite having about the same line averaged density, the density profiles in the two discharges are different. The electron pressures in the centre are therefore different even though the central electron temperatures are similar. These results indicate that the confinement improvement affects at least the electron transport. A further indication of this comes from the comparison between the measured stored electron energy and the prediction from the Rebut-Lallia-Watkins scaling law [13], Fig. 1b.

Another interesting observation is that the plasma rotation velocities differ significantly between the two discharges, Fig. 1c, The rotation velocities are measured by the Doppler shift of the Fe^{24+} line [14]. Owing to the strong parallel friction forces present in the highly collisional plasmas considered here, the toroidal rotation speeds of the main ions and the impurities are expected to be approximately the same [15]. In the case of the high concentration discharge, the plasma accelerates in the co-current direction during the application of ICRF power and reaches a toriodal velocity of 40 km/s. In contrast, the low concentration discharge accelerates in the counter current direction and reaches a toroidal velocity of about −15km/s.

2.3 Scaling studies

In order to get an overview of the influence of hydrogen concentration and the ion heating on the performance of Tore Supra discharges, we have analysed a number of discharges with varying minority concentrations. Data taken at various time points within these discharges are displayed in Figs. 3-5. In Fig. 3, the central ion pressure is shown as a function of $n_H n_e / \sqrt{T_e}$. The reason for choosing this x-axis variable is that it is almost proportional to $P_{RF} E_c / \langle E_{H,fast} \rangle$ (the averaged energy of the fast hydrogen ions, $\langle E_{H,fast} \rangle$, is approximately proportional to $P_{RF} t_s / n_H$, where t_s is the ion electron slowing down time in the centre of the plasma;

$E_c = 0.5mv_c^2$). Since the fraction of bulk ion heating depends crucially on the ratio $E_c / \langle E_{H,fast} \rangle$, the total bulk ion heating should scale strongly with this ratio multiplied with the RF-power. As can be seen, there is a clear scaling of the ion pressure with $n_H n_e / \sqrt{T_e}$. Owing to the fact that it is the hydrogen concentration that by far has the greatest variation of the variables on the x-axis, from 2 to 7%, Fig. 3 gives a clear indication of the influence of the hydrogen concentration on the bulk ion heating efficiency.

The measured toroidal rotation velocity is shown as a function of the central ion pressure in Fig. 4. The correlation between the toroidal velocity and the ion pressure is very strong. This trend, apart from the fact that also negative rotation is seen in Tore Supra, is strongly reminiscent of the scaling found for the toroidal rotation during ICRF heated H-modes in JET [16] and C-MOD [17, 18]. However, the correlation between the ion pressure and the rotation velocity does not necessarily imply that the fp_i / fr is the dominating term in the expression for the rotation velocity, which for a plasma species (assuming the poloidal rotation velocity to be small) can be written as, $v_\varphi = -(1/n_j Z_j e) fp_i / fr + E_r / B_\theta$. Instead it could be that the radial electric field also scales with the ion pressure. In Fig. 5, the H factor, i.e. the stored energy normalised to the ITER-L97 scaling law [12], is plotted as a function of the central rotation velocity. As can be seen, the H factor appears to be strongly linked to the rotation. This suggest that the rotation could have played a role in suppressing the turbulence underlying the transport in these discharges. On the other hand, it is also possible that the increased rotation velocity is just a consequence of the improved confinement and/or higher ion heating fraction. One must therefore be cautious in drawing any firm conclusions from the present data. There are many possibilities for explaining the observations.

3. NUMERICAL SIMULATIONS

The two discharges in section 2.2 have been simulated numerically. To get a general overview of the power deposition profile the relative fractions of bulk ions and electron heating etc. we have used the PION code [19]. Owing to the fairly large ripple in Tore Supra it is also necessary to consider the influence of ripple losses. Calculations of such losses are not only of importance for estimating the power lost from the plasma, but also for finding the fast ion current induced by them. This current will have an influence on toroidal momentum balance in the plasma. We have studied the ripple losses with the FIDO code [20], which solves a 3D orbit averaged Fokker Planck equation with a Monte Carlo method. In order to account for the ripple, we have introduced a ripple losses model in the code which is similar to the one outlined in Ref. [21].

The result of the PION simulations, during the steady phase of the discharges, for the bulk electron and ion heating (collisional power transfer from the resonation ions and direct absorption of the ICRF power), is shown in Fig. 6. As can be seen the bulk ion and electron heating are very close to each other for the high concentration discharge #TS21044, whereas electron heating dominates strongly for the low concentration discharge #TS23967. If we look at the average energy of the resonation hydrogen ions in the simulations, we find that a maximum of 180 keV is reached for the low concentration discharge, well above the critical energy, whereas only 50 keV is reached for the high concentration discharge, i.e. in the region around the critical velocity. These results are consistent with the experimental observations, and strengthen the conclusion that the hydrogen concentration plays an important role for the level of ion heating achieved in the considered discharges.

The wave field pattern used in the FIDO code for the ripple loss studies has been adjusted so that the power deposition becomes, within reason, consistent with that of the PION code. The result of the FIDO calculations show that the ripple losses due to ripple well trapping are around 8% for the two discharges whereas the direct losses, caused by a combination of large orbit width and stochastic ripple diffusions, are significantly higher for the low concentration case, around 10%, than for the high concentration case, around 3 %. Thus, the actual power input to the bulk plasma is somewhat lower for the low concentration case because of the ripple losses. However, it should be noted that the power scaling in the ITER-L97 scaling law

is $P^{0.25}$. Hence, a 5-10% difference in bulk heating power has only a modest effect on the relative prediction of the stored for the two discharges. Another important issue is the toroidal momentum imparted to the plasma because of the fast ion losses. Such losses give rise to a momentum in the counter current direction. There are two components, first there is the radial current of fast ions. In order to maintain quasi-neutrality, this current is compensated for in the bulk plasma by an inward current. The $\vec{j} \leftarrow \vec{B}$ force due to this current gives momentum to the background plasma in the counter current direction. By estimating the radial fast ion current and integrating the $\vec{j} \leftarrow \vec{B}$ force across the plasma we can obtain a rough figure for the momentum imparted to the background plasma. The other component is due to the direct losses. The toroidal velocity of the trapped ions intersecting the wall is always in the counter current direction. Consequently, there will be a counter current momentum lost from the plasma because of the direct losses. However, this momentum turns out to be much smaller than that due to the radial fast ion current for the discharges considered here. The simulated momentum input for the two discharges turn out to be of the same order, around 0.5 – 1 Nm in the counter current direction. It should be noted that that the radial fast ion current associated with the stochastic losses is relatively small since only very energetic ions are affected by this process.

4. DISCUSSION AND CONCLUSION

The ICRF heating experiments carried out in Tore Supra with various concentrations of the absorbing minority species show clearly that the ion heating increases with the concentration of the minority species. The basic explanation for this is that the higher concentration lowers the averaged energy of the resonating ions, bringing it closer to or below the critical energy.

The improved level of ion heating is accompanied by other effects. For instance, the bulk plasma rotation seems to be strongly influenced by the bulk ion pressure. In the case of low concentration the plasma rotates in the counter current direction. In discharge #TS23967 the rotation velocity was about –15 km/s. If we assume that the momentum confinement time is of the order of the energy confinement time (around 0.15 sec) and that the whole plasma

rotates with the same angular frequency we obtain a momentum input necessary to sustain the rotation of the order of 0.3 Nm. This is the same order of magnitude as we find from the simulations of the ripple losses. Thus, the counter rotation can be explained by fast ion losses, which is consistent with earlier observations made on Tore Supra [22]. The positive rotation observed for the high concentration cases, on the other hand, is much more difficult to explain. Since dipole phasing of the ICRF antennas was used in the experiments reported here, the momentum input from the waves to the plasma should have been very small. Furthermore, no significant difference in the calculated input momentum due to fast ions losses was found. A possibility is therefore that the rotation is related to the behaviour of the bulk plasma. The strong correlation between the rotation velocity and the bulk ion pressure is an indication of this.

The global energy confinement of the plasma has also been found to improve in discharges with a higher fraction of ion heating. This improvement is seen not only in the ion transport channel but also in the electron one. Furthermore, there appears to be a strong correlation between the confinement improvement and the rotation velocity, suggesting a link between the confinement and the rotation. The exact cause of the improved confinement remains, however, to identified.

Acknowledgement

It is a pleasure to thank our colleagues at Tore Supra who have operated the tokamak, the heating systems and the diagnostics during the experiments reported here. We would also like to thank Drs. X. Garbet and A. Bécoulet for fruitful discussions.

References

[1] Start, D., et al., Nuclear Fusion **39** (1999) 321.

[2] Phillips, C.K., et al., Physics of Plasmas **2** (1995) 2427.

[3] Hoang, G.T., et al., Nuclear Fusion **40** (2000).

[4] Bergeaud, V., Eriksson, L.-G., Start, D.F.H, Nuclear Fusion **40** (2000) 35.

[5] Equipe Tore Supra (presented by R. Aymar), in Plasma Physics and Controlled Nuclear Fusion Research, Proceedings of the 12th International Conference, Nice, 1988 (IAEA, Vienna, 1989), Vol. 1, p. 9.

[6] Stix, T.H., Nuclear Fusion **15** (1975) 737.

[7] Adams, J.M., Nuclear Fusion **31** (1991) 891.

[8] Zweben, S.J. et al., Nuclear Fusion **32** (1992) 1823.

[9] Bhatnagar, V.P., et al., Nuclear Fusion **33** (1993) 83.

[10] M. Fois, G.T. Hoang, T. Hutter., Controlled Fusion and Plasma Physics (Proceedings of the 14th European Physical Society Conference on Controlled Fusion and Plasma Heating, Madrid, 1986), Vol 17C, Part I, European Physical Society (1993) 1693.

[11] Tore Supra Team (presented by B. Saoutic) Fusion Energy, Edited by IAEA Vienna (1997), Vol 1, p. 141.

[12] Kaye, S.M, ITER Confinement Database Working Group, Nuclear Fusion **37** (1997) 1303.

[13] Rebut, P.H., Lallia, P.P., Watkins, M.L., in Plasma Physics and Controlled Nuclear Fusion Research (Proceedings of the 12th International Conference, Nice 1998) Vol II, IAEA Vienna (1989) 191.

[14] A. Romanikov, et al., Nucl. Fusion, **40** (2000) 319.

[15] Kim, Y.B., Diamond, P.H., Groebner, R.J., Phys. Fluids B 3 (1991) 2050.

[16] Eriksson, L.-G., Righi, E., Zastrow, K.D., Plasma Physics and Controlled Fusion **39** (1997) 27.

[17] Rice, J.E., et al., Nuclear Fusion **38** (1998) 75.

[18] Hutchinson, I.H., et al., In Controlled Fusion and Plasma Physics (Proceedings of the 27th European Physical Society Conference on Plasma physics and controlled fusion, Budapest, Hungary, 2000) European Physical Society, Geneva 2000, paper P4.043

[19] L.-G. Eriksson, T. Hellsten and U. Willén, Nucl. Fusion **33** (1993) 1037.

[20] J. Carlsson, T. Hellsten and L.-G. Eriksson, in Proceedings of the Joint Varenna Lausanne Workshop on 'Theory of Fusion Plasmas' 1994 (Editrice Compositori, Bologna, 1994), p. 351.

[21] Putvinskij, S., et al., Nuclear Fusion **34** (1994) 495.

[22] Platz, P., et al., in Controlled Fusion and Plasma Physics (Proceedings of the 22nd European Physical Society Conference on Plasma physics and controlled fusion, Bournemouth, 1995), Vol. 19C, Part III, European Physical Society, Geneva (1995) p. 337.

Proposed classification:

G2, Te; G2, Ti, F1, Te; F2, Ti; F3, Ti

Figure captions

Fig. 1 Overview of two discharges, TS#21044 (left) and TS#23967 (right), with different hydrogen concentrations and similar ICRF power levels; (a) line averaged electron density together with the ICRF power, (b) central ion and electron temperatures (c) total stored energy, energy stored in the electrons and L-mode predictions (ITER-L97 [10] for the total stored energy and Rebut-Lallia-Watkins [11] for the electron stored energy), (d) the central toroidal rotation velocity, (e) the estimated hydrogen concentration.

Fig. 2 The electron pressure profiles for discharge TS#21044 and TS#23967.

Fig. 3 The central ions pressure as a function of $n_H n_e / \sqrt{T_{e0}}$, a parameter which scales strongly with the bulk ion heating power.

Fig. 4 Variation of central rotation velocity as a function of the central ion pressure.

Fig. 5 The H factor, i.e. the stored energy normalised to the ITER-L97 scaling law [10], as a function of the central rotation velocity.

Fig. 6 Simulated power densities going to bulk ion (full curves) and electron (dashed curves) heating during the steady state phase for TS#21044 (a) and TS#23967 (b).

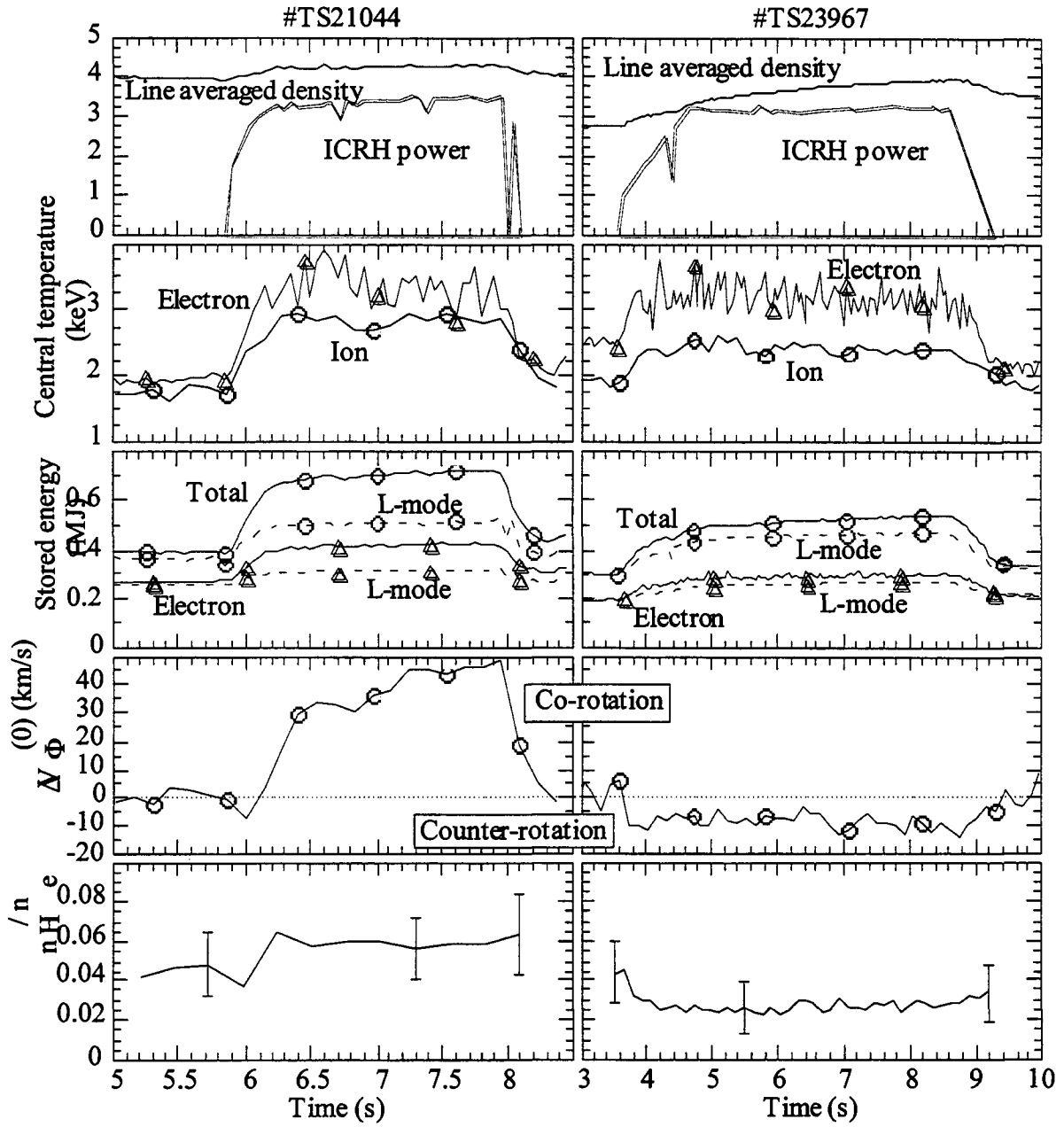
#TS21044
#TS23967
Line averaged density
ICRH power
Central temperature (keV)
Electron
Ion
Stored energy (MJ)
Total
L-mode
Electron
Δ V Φ (0) (km/s)
Co-rotation
Counter-rotation
n e / n H
Time (s)

Figure 1

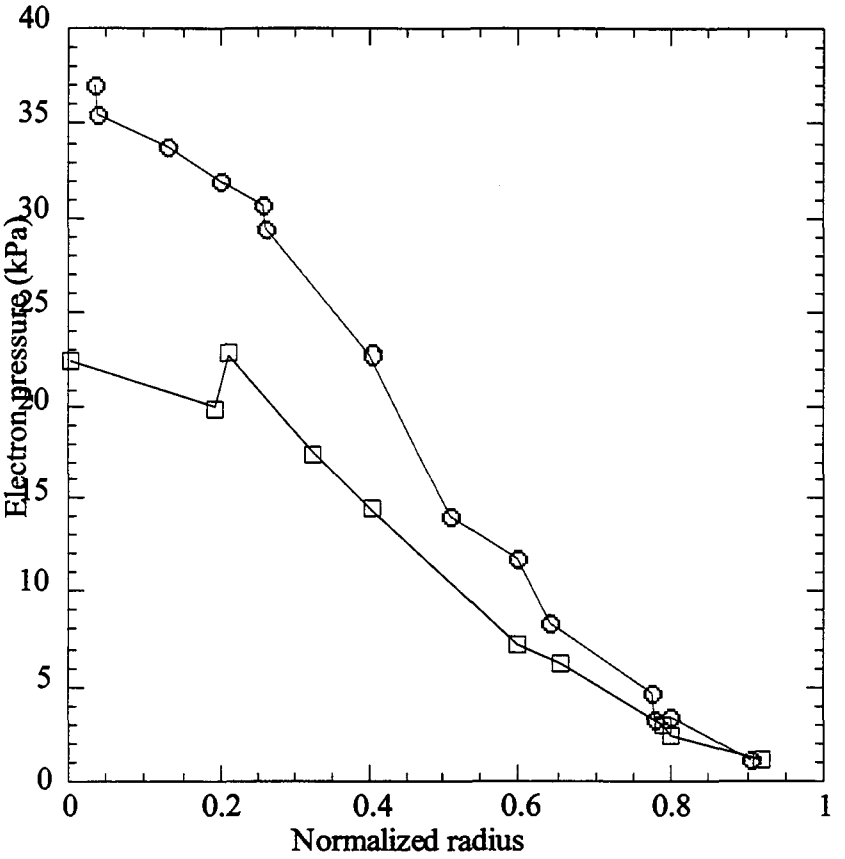
40
35
30
25
20
15
10
5
0
Electron pressure (kPa)
0
0.2
0.4
0.6
0.8
1
Normalized radius

Figure 2

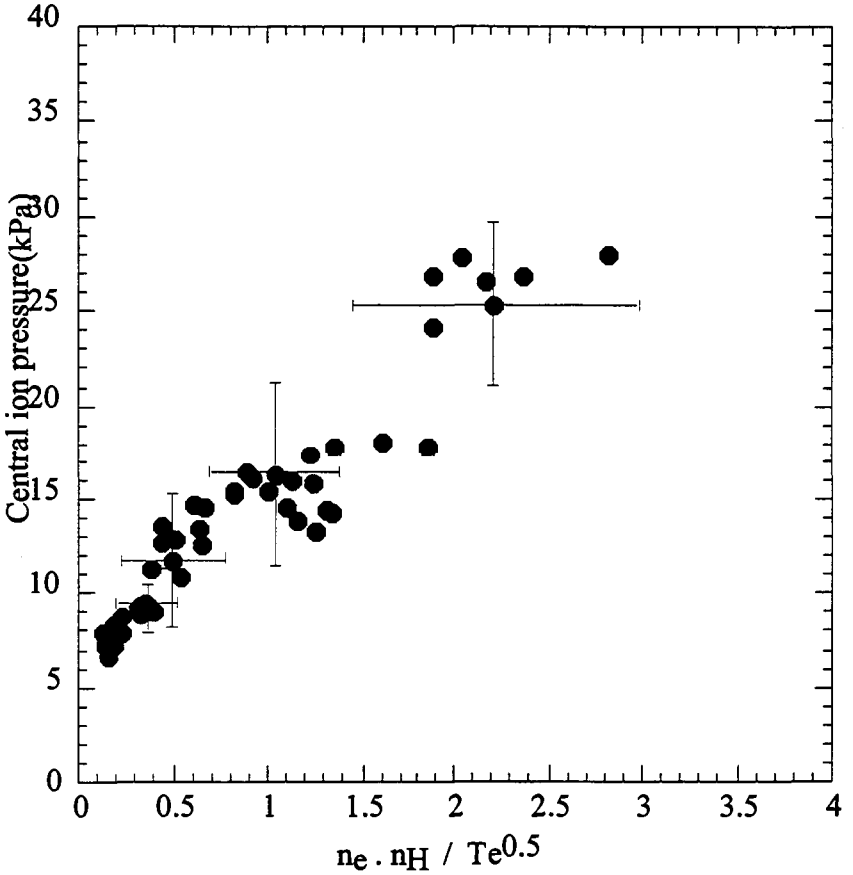
Central ion pressure(kPa)
40
35
30
25
20
15
10
5
0
0
0.5
1
1.5
2
2.5
3
3.5
4
$n_e \cdot n_H / Te^{0.5}$

Figure 3

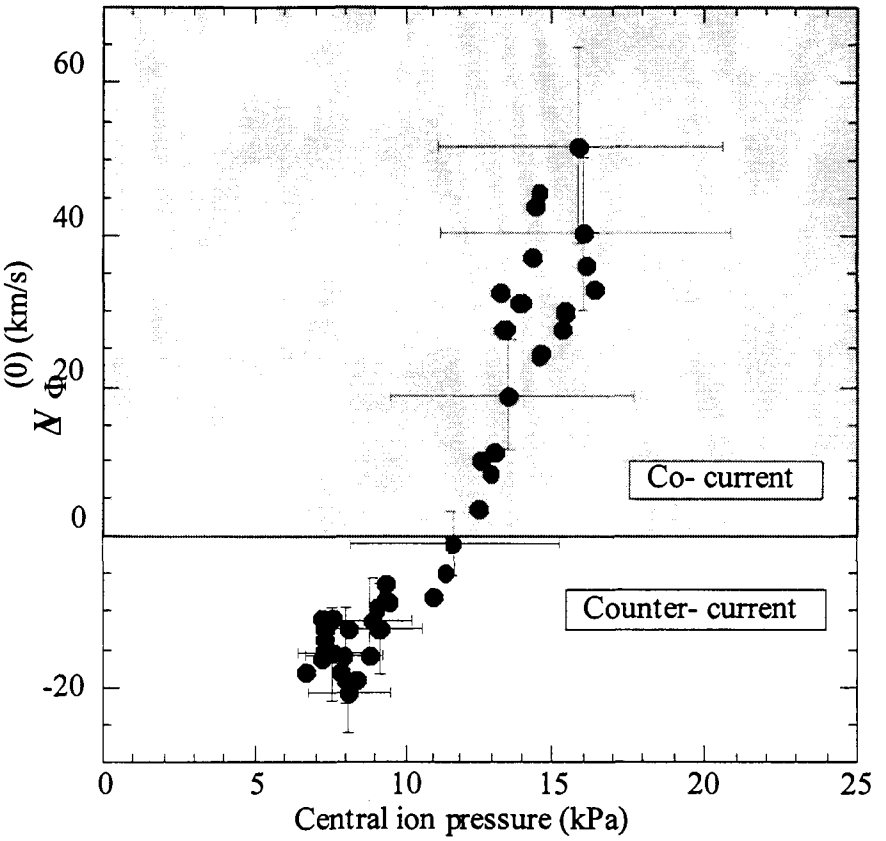
60
40
20
0
-20
0
5
10
15
20
25
Central ion pressure (kPa)
(0) (km/s)
Co- current
Counter- current

Figure 4

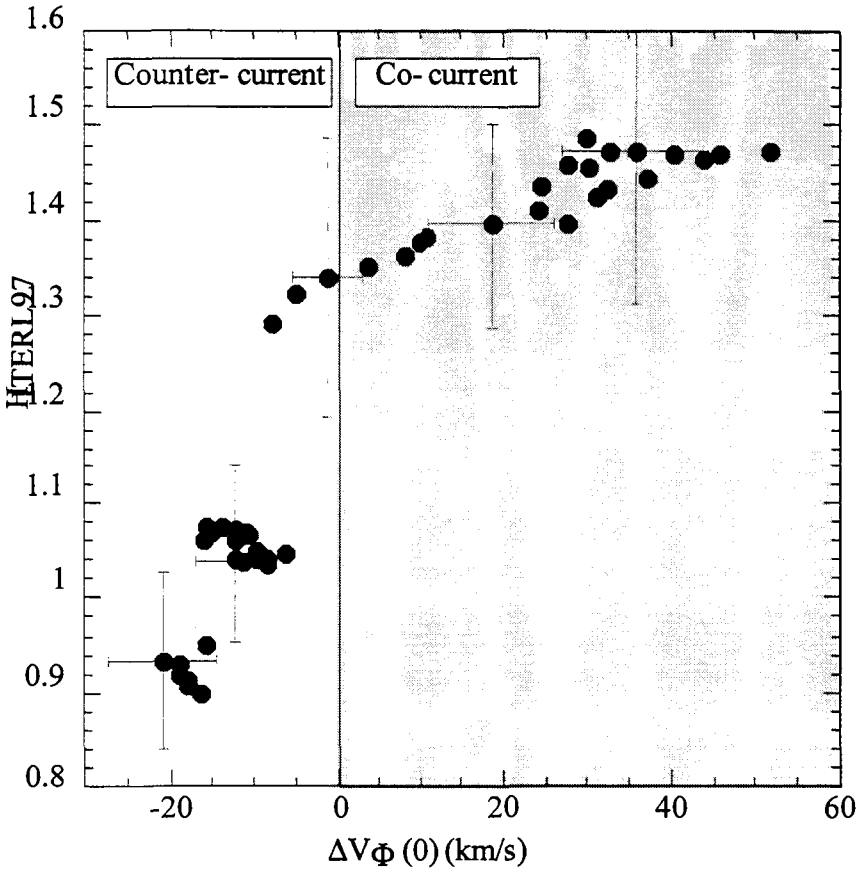
Counter- current
Co- current
HTERL97
ΔVΦ (0) (km/s)
1.6
1.5
1.4
1.3
1.2
1.1
1
0.9
0.8
-20
0
20
40
60

Figure 5

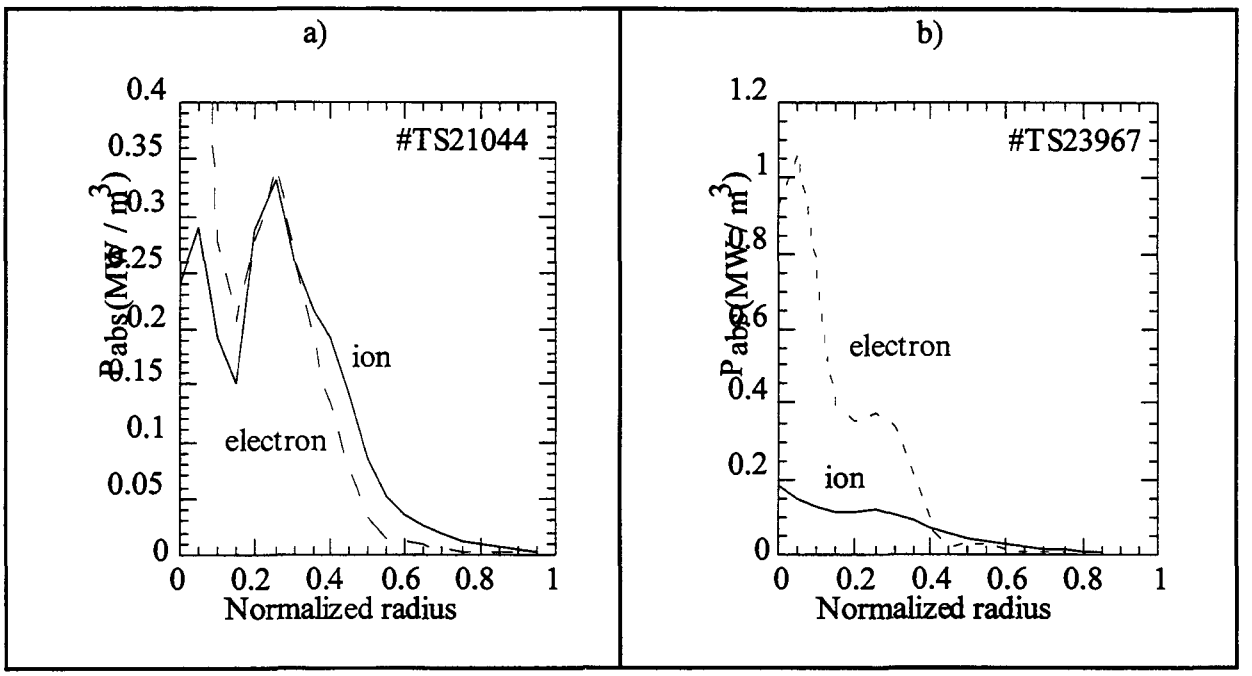
a)
#TS21044
ion
electron
Normalized radius
b)
#TS23967
electron
ion
Normalized radius

Figure 6